Production of Nanostructured Materials via Uniform Melt State Process

M. Redjdal*, K. Hadidi*, R. A Ristau** and S. K. Sundaram***

*Amastan LLC, Storrs, CT, USA, mredjdal@amastan.com
**Institute of Materials Science, University of Connecticut, Storrs, CT, USA
***Kazuo Inamori School of Engineering, Alfred University, Alfred, NY, USA

ABSTRACT

We have produced and characterized high phase purity amorphous yttrium-aluminum garnet (a-YAG) powder using the UniMelt™ process. This process consists of axial injection of uniformly sized solution precursor droplets into an axisymmetric microwave plasma-generated hot zone with uniform temperature profile and laminar flows with high heating and quenching rates, leading to a high purity powder, and hence homogenous phase microstructure. The powders are spherical shells of a-YAG. Subsequent atmospheric thermal heating to 1200°C for 1 hour of the amorphous powder produces a cubic and homogeneous nanocrystalline YAG microstructure with high phase purity and crystal grains size averaging 100 nm. The calcined shells have an estimated thickness of few crystalline grains.

Keywords: microwave, plasma, Unimelt, YAG, laser, pyrolysis.

1 INTRODUCTION

Optical ceramic yttrium-aluminum garnet (YAG) as laser gain material has seen an increasing demand as a substitute to single crystalline YAG due to its advantages in terms of fabrication, design and cost without any reduction in performance [1]. Single crystal YAG is grown from molten YAG to form a crystal boule using the Czochralski method [2]. Growing larger crystals for complex laser designs is mass limited because of fracture, and the introduction of stress and index distortions [3]. With the advent of new consolidation techniques, fabrication of nanostructured YAG powders solves all these issues. YAG ceramic as laser material offers many advantages over its YAG single crystal counterpart, in terms of: (1) Ease of fabrication; (2) Less expensive; (3) Fabrication of large size and high dopant concentration; and (4) Mass production [4]. The leading YAG nanopowder producer for laser applications is Konoshimu Chemical Company in Japan (see Japanese Patents [5, 6]). YAG nanopowders are produced using a co-precipitation method, which involves chloride precursors as sources for aluminum and yttrium, arduous titration, several steps of washing and drying before calcining several times at 1200°C to obtain YAG powder, which is then milled for consolidation into a near-net shape microstructure [4]. One major drawback according to Sang and coworkers [7] is that the method suffers from the difficulty to control the composition uniformity of the precursor because of the different solubility product constants of Y^{3+} and Al^{3+} solutes. Other methods include sol-gel [8] and flame combustion [9].

In this work, we apply a new pyrolysis method using microwave generated plasma with axial injection of solution precursors to produce homogeneous amorphous YAG which is subsequently calcined to lead to nanocrystalline YAG. The precursor uses aluminum and yttrium nitrates that are homogeneously dissolved in distilled water and solvents. Size of particles, morphology, purity and homogeneity of phase microstructure are analyzed using scanning electron microscopy (SEM), energy dipsersive x-ray (EDX), x-ray diffraction (XRD), and transmission electron microscopy (TEM) techniques.

2 EXPERIMENTAL SET UP

Stoichiometric amounts of yttrium (Alfa-Aesar, 99.9%), and aluminum (Alfa-Aesar, 98%) nitrate salts are dissolved in distilled water and mixed in a complexing network of citric acid (Alfa-Aesar, 99^{+}%) and ethylene glycol (Fisher Scientific, 99%). The salt route is relatively cheap as the reactant sources are low cost and readily available. Yttrium and aluminum salts possess high miscibility liquid phases and low melting points (<100 °C) that lead to high level of precursor homogeneity [10]. With appropriate concentration of chelating reagents, this mixture allows an excellent dispersion of Y^{3+} and Al^{3+} ions in the solution through thorough dissolution of salts along with increased solution stability [11].

The well-stirred precursor is injected axially as uniformly sized droplets using a piezo-driven droplet maker [12, 13]. The voltage and frequency of the exciting signal of the piezoelectric element are tuned to generate a stable and uniform droplet stream, with a droplet diameter of 100 µm. Each droplet undergoes uniform pyrolysis in the UniMelt™ process [14, 15] characterized by an axisymmetric hot zone with uniform temperature profile and laminar flows along with high heating and quenching rates. Optimized experimental parameters consist of microwave power, solution precursor injection flow rate, and carrier gas flow rate inside the plasma hot zone necessary to maintain a stable plasma. The product is quenched into atmospheric environment. YAG particles are collected in a stainless steel filter with 10 µm pore diameter.

The YAG particles are analyzed for size, size distribution, texture, and morphology using SEM (JEOL 6335F) analysis. To investigate phase homogeneity, purity,

and crystalline grain growth with temperature, the powder particles are calcined up to 1200°C in a pressurless environment and analyzed using XRD (Bruker D2 Phaser), and TEM (FEI Tecnai T-12 TEM/STEM) techniques.

3 RESULTS AND DISCUSSION

Figure 1 shows that the resulting YAG particles are nearly spherical, shell-like, with a porous texture at the surface. The diameter varies over 300- 400 µm, or four times the size of the injected precursor droplet. The shell particles obtained tend to expand and are fluffy due to the behavior of nitrate precursors used in the process [16]. The shell particles are easily breakable into platelets.

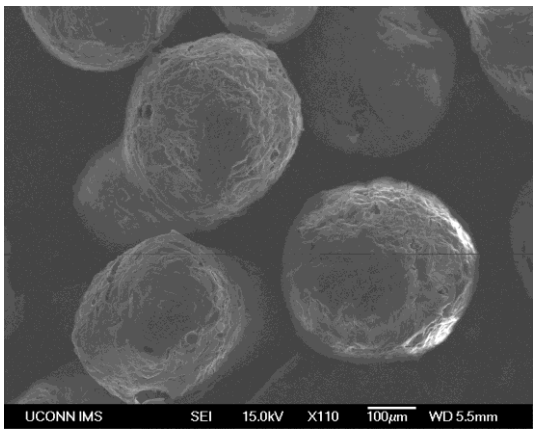

Figure 1. SEM image of yttrium-aluminum-garnet powder particles obtained using the UniMelt™ process.

XRD analysis was used to investigate the phase microstructure of the particle product which was found to be mostly amorphous as shown in Figure 2. Furthermore, three broad wide peaks can be seen which would suggest the presence of possible embedded nanocrystalline phases in the overall amorphous YAG. However, selective area diffraction pattern (SADP) shown here as an inset in Figure 2, confirms the amorphous nature of the YAG powder.

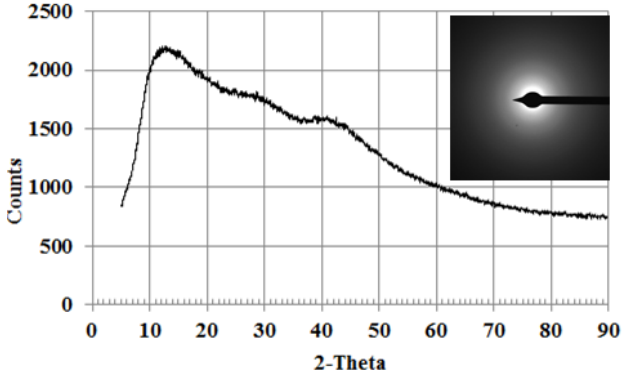

Figure 2. XRD plot and SADP pattern (inset) of YAG powder produced using the UniMelt™ process showing total amorphous microstructure.

The powders were subsequently calcined at 950°C for one hour, analyzed using XRD, and compared to the crystalline structure of YAG (JCPDS Card No. 33-0040) [17]. The intensity of the peaks in the reference card was scaled accordingly for better visual comparison at corresponding angles. It can clearly be seen in Figure 3 that there is a good match between most of the major and small peaks in the XRD plot of the UniMelt-processed and calcined YAG and crystalline YAG used as reference. The SADP shown as an inset in Figure 3 indicates that two phases could be present, one amorphous and the other crystalline identified by a diffuse pattern of two distinct rings observed. No monoclinic yttrium aluminum YAM ($Y_4Al_20_9$) or yttrium aluminum perovskite YAP ($YAlO_3$) can be detected in these powders. However, three minor peaks remain to be identified at 2Θ equal to 17.2°, 44.7°, and 49.5°. On calcination at higher temperature, these peaks resolve into crystalline YAG. Fully resolved crystalline YAG requires calcination up to 1100°C. It must be pointed out that YAM has a small peaks at 17.562° (intensity=1/total=100), 44.210° (9/100), 49.354° (19/100), and 49.757° (17/100) on a maximum scale value of (100/100) according to JCPDS Card No. 34-0368. On the other hand, YAP exhibits peaks at 44.181° (8/100), 49.029° (31/100), and 49.429° (18/100) according to JCPDS Card No. 33-0041. As the main objective of this effort is to demonstrate first the synthesis of YAG, only moderate quality commercial yttrium and aluminum nitrates have been used, i.e., 99.9% and 98%, respectively. As the UniMelt process is a homogenous pyrolysis process, it is clear that higher purity nitrates would lead to higher phase purity YAG.

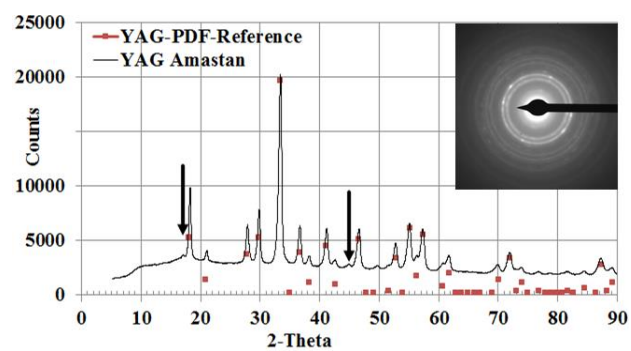

Figure 3. Comparison of XRD of calcined yttrium-aluminum-garnet (solid line) to YAG (JCPDS 33-0040, squares); SADP are included as inset.

Calcination at high temperature allows the investigation of grain growth versus temperature and the determination of phase distribution of yttria and alumina components in the YAG microstructure. The resulting microstructure of the powder particles calcined at 950ºC for 1 h at atmospheric pressure were observed using TEM analysis and is shown in Figure 4. Two phases are present, one crystalline (dark contrast) and the other amorphous (white grains). Only dark grains changed contrast as they were observed under

different diffraction angles. Both phases are embedded in thin sheets, two of them shown in circles, and other sheets can be observed in the vicinity. Observation of several of these sheets under different angles showed that they are semi-spherical to round in shape and about 1 grain in thickness. This observation also allowed identification of the amorphous grains, as they remained identically bright in color as the diffraction angle changed. The grains measure between 15 and 30 nanometers (nm), whereas the sheets are 2D platelets that can be as large as 150 nm. These sheets where obtained from sonicating the shells shown in Figure 1. Calcination of the powder at temperature as high as 1100°C is required to fully crystallize the YAG powders.

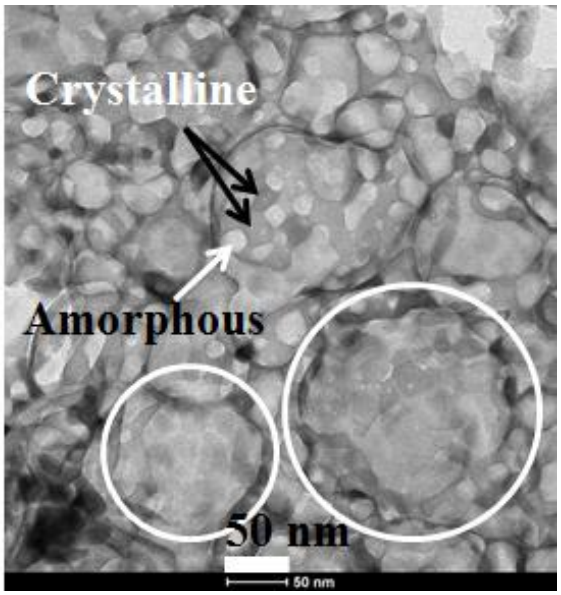

Figure 4. TEM of YAG powder calcined at 950°C for 1 hour showing a mix of crystalline (dark) and amorphous phases (bright regions).

This powder was further calcined at 1200°C for one hour to remove all remaining amorphous phases observed in Figure 3 and Figure 4, and analyzed using XRD technique. As shown in Figure 5, the resulting crystalline structure (solid line) is compared again to the crystalline structure of YAG (JCPDS Card No. 33-0040, squares) [17]. The intensity of the peaks in the reference card was scaled accordingly for better visual comparison at corresponding angles. It can clearly be seen that there is a perfect match between the most of the major and small peaks in the XRD plot of the UniMelt-processed and calcined YAG and crystalline YAG used as a reference. The perfect alignment of all the peaks denotes the phase purity of the resulting YAG free of any other phases of YAM, or YAP, in the binary Y_2O_3-Al_2O_3 oxide system. This phase purity is determined to be pure to the detection limit of XRD technique estimated statistically to be about 5 volume % [18].

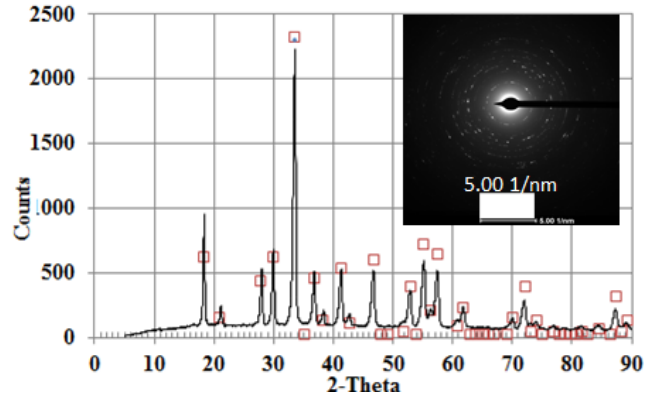

Figure 5. Comparison of XRD spectra of Amastan's YAG (solid line) calcined at 1200°C to YAG (JCPDS Card No. 33-0040, in squares); SAD patterns of the calcined power are included as insert.

Careful measurements of SADP of a large number of particles of the powder calcined at 1200°C were also performed. These results are shown in the inset of Figure 5. As can be seen, a pattern of rings was obtained and the lattice spacing of the first six was measured and compared to that of cubic $Y_3Al_5O_{12}$. The resulting values are shown in Table 1. The lattice spacing measured from the SADP match very well with cubic $Y_3Al_5O_{12}$. This is further evidence that the calcined powder produced using UniMelt has the cubic microstructure of YAG as was inferred by the XRD spectrum in Figure 5.

Table 1. Lattice spacing measured from SADP rings of Amastan's YAG powder and compared to cubic $Y_3Al_5O_{12}$.

Ring Number	Measured d (nm)	Calculated d (nm)
1	0.488	0.490
2	0.423	0.424
3	0.380	0.379
4	0.319	0.321
5	0.298	0.300
6	0.268	0.268

TEM analysis was performed on the powder calcined at 1200°C and the result is shown in Figure 6. Three different orientations of the TEM beam with respect to the crystals were chosen to determine contrast in the YAG crystals and consequently possible phase segregation in these crystals. The average size of the grains is estimated to be 100 nm. All the grains, in particular grains indicated as 1, 2, and 3, in Figure 6a, exhibit an observable change in color contrast as the orientation of the beam was changed in Figure 6a,b, and c. For instance grain 1 is shown dark in Figure 6a, then dark-to-light gray in Figure 6b, and light gray in Figure 6c. The bright-dark condition is due only to the orientation of the beam with the crytal grain and not to different composition in the crystal grain. It does not preclude that differences in composition may exist. However, TEM results indicate that the calcined sample is fully crystalline.

EDX (not shown) analysis of many of these crystals showed that they have aluminium (Al), yttrium (Y), and oxygen (O). No distinct regions of Al, Y, and O were detected even in clearly separated single particles. This would indicate that the elements Al, Y, and O are distributed homogeneously in the YAG nanostructure produced using UniMelt™. EDX analysis confirms that the average composition of the 1200°C calcined sample is close to that of YAG.

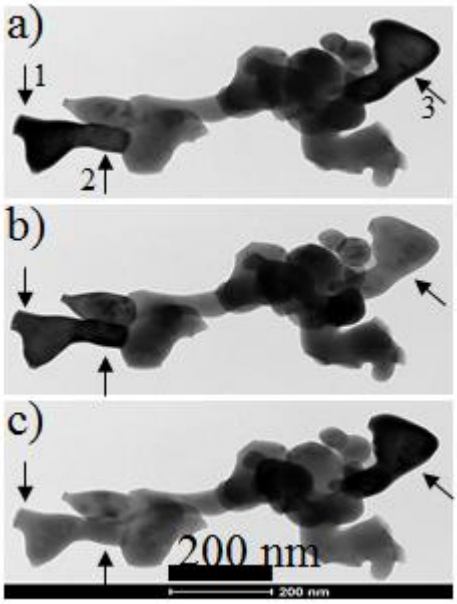

Figure 6. TEM image of calcined powder at 1200°C observed under three different beam-scattering conditions showing contrast change in YAG crystals.

4 CONCLUSION

The UniMelt™ process provides a novel synthesis method for manufacturing phase-pure composite materials, combining compositional homogeneity through uniform precursor droplet injection with uniform thermal paths. It has been used to produce spherical YAG particle powders with nearly uniform size and morphology, and amorphous microstructure. Upon calcination at 1200ºC, the particles crystallized as a phase-pure cubic nanocrystalline YAG.

Acknowledgments: We would like to thank Professor Eric Jordan at UConn for facilitating access to SEM, TEM, and XRD apparatus.

REFERENCES

[1] J. Huie and R. Gentilman, “Characterization of Transparent Polycrystalline Yttrium Aluminum Garnet (YAG) Fabricated from Nano-powder”, Proceedings of SPIE, Vol. 5786, Window and Dome Technologies and Materials IX, 251-257, 2005.

[2] (Polish), (English), Paweł Tomaszewski, ""Jan Czochralski i jego metoda" (ang. Jan Czochralski and his method), Oficyna Wydawnicza ATUT, Wrocław–Kcynia, 2003.

[3] J. Huie and R. Gentilman, “YAG Solid State Laser Ceramics Breakthroughs at Raytheon”, Raytheon Technology Today, issue 2, 26-28, 2010.

[4] J. Lu, K.-I Ueda, H. Yagi, T. Yanagitani, Y. Akiyama, and A. A. Kaminskii, “Neodymium Doped Yttrium Aluminum Garnet ($Y_3Al_5O_{12}$) Nanocrystalline Ceramics—A New Generation of Solid State Laser and Optical Materials”, Journal of Alloys and Compounds, 341, 220–225, 2002.

[5] T. Yanagitani, H. Yagi and M. Ichikawa, Japanese patent: 10-101333, 1998.

[6] T. Yanagitani, H. Yagi and Y. Hiro, Japanese patent: 10-101411, 1998.

[7] Y. Sang, H. Liu, Y. Lv, J. Wang, T. Chen, D. Liu, X. Zhang, H. Qin, X. Wang and R. I. Boughton, “Yttrium aluminum garnet nanoparticles synthesized by nitrate decomposition and their low temperature densification behavior”, Journal of Alloys and Compounds, 490, 459–462, 2010.

[8] L. Yang, T.C. Lu, H. Xu, and N. Wei, “Synthesis of YAG Powder by the Modified Sol–gel Combustion method”, J. Alloys Compd., 484, 449–451, 2009.

[9] R. M. Laine and S. C. Rand, AFOSR Report, 2007. (www.dtic.mil/dtic/tr/fulltext/u2/a475246.pdf)

[10] M. Nyman, J. Caruso, M. J. Hamden-Smith and T. T. Kodas, J. Am. Ceram. Soc., 80, 1231-1238, 1997.

[11] S. Gupta, and R. S. Katiyar, R “?”, J. Raman Spectrosc., 32, 885–891, 2001.

[12] Lord Rayleigh, “On the Instability of Jets”, Proc. of the London Math. Soc., Vol. 10, No. 1, 4-12, 1879.

[13] M. Orme and E. P. Muntz, "The Manipulation of Capillary Stream Breakup Using Amplitude Modulated Disturbances: A Pictorial and Quantitative Representation," Phys. of Fluids, Vol. 2, no. 7, 1124–1140, 1990.

[14] K. Hadidi, B. M. Cetegen, E. H. Jordan and P. Woskov, “Microwave Plasma Apparatus and Method for Materials Processing”, Pub. No.: US 2008/0173641 A1, 2008.

[15] M. Redjdal, K. Hadidi, E.H. Jordan, O.A. Graeve, and C.M. Brunet, “Uniform Melt State Process™ for the Production of Nanostructured Composite Powders”, 14th DOD Electromagnetic Windows Symposium, San Antonio, May 2012.

[16] G. L. Messing, S.-C. Zhang and G. V. Jayanthi, “Ceramic Powder Synthesis by Spray Pyrolysis”, J. Am. Ceram. Soc., 76 [11], 2707-25, 1993.

[17] International Centre for Diffraction Data, Newtown Square, PA. (http://www.icdd.com/)

[18] J. R. Connolly, “Introduction Quantitative X-Ray Diffraction Methods”, for EPS400, Spring 2012.